

MODELING AND PERFORMANCE ANALYSIS OF A PV-POWERED WATER PUMPING
SYSTEM INSTALLED AT EL-MANSOURA CITY , EGYPT

نمذجة وتحليل أداء منظومة ضخ مياه منقذاه كهربوضوئيا مقامة بمدينة
المنصورة جمهورية مصر العربية

BY

M.A. El-Sayes M.H. El-Maghraby I.I.I. Mansy A. Ibrahim

Faculty of Engineering - University of El-Mansoura

Electrical Power and Machines Dept., El-Mansoura, Egypt.

الخلاصة : يحلل البحث أداء أربعة أشكال مختلفة لمنظومة ضخ مياه تغذى من مصفوفة خلايا
كهربوضوئية وهذه المنظومة مقامة بالمنصورة بجمهورية مصر العربية وتضم
منظومة ضخ المياه على محرك تيار مستمر بمغناطيس دائم يدبر مضخة مياه طرد
مركزي ويغذى المحرك من مصفوفة خلايا كهربوضوئية إما مباشرة أو عن طريق بطارية
تخزين أو حاكم أو بطارية تخزين موصلة بحاكم على التوالي وهذه هي الاشكال الأربعة
لنظومة ضخ المياه المدروسة بالبحث ويستخرج المبحث نماذج رياضية جديدة تعبر
عن معدل سريان المياه كدالة في خصائص مكونات منظومة ضخ المياه وخصائص الموقع
المقام عليها النظام هذه النتائج مستنبطة من القياسات السأخوذة بالموقع وقد
تم مقارنة نتائج تلك النماذج بالأخرى المستنتجة من تحليل المنظومة رياضيا .

ABSTRACT

This paper investigates the performance of four different configurations of a photovoltaic powered water pumping system (PVEWPS). This system involves a permanent magnet direct current motor. This motor drives a centrifugal pump on the same shaft. The motor-pump set is powered from a photovoltaic cells array (PVCA) either directly or through one of the storage battery (SB), controller and SB in series with a controller.

This work presents performance analysis of the proposed configurations. Also, this paper gives water flow rate model as a function of the system components characteristics and the environmental circumstances.

This paper introduces a mathematical model by using theoretical analysis and experimental recorded data. Then, this work presents comparison between the two models.

This research gives the obtained results and final conclusions.

Received in 8/8/1994

1-INTRODUCTION

The feasibility of using photovoltaic array to drive water pumping units for irrigation and drinking water in remote areas, where other energy sources are not available, has already been demonstrated. New processes for manufacturing photovoltaic cells and enhancing their conversion efficiency are currently being explored and aimed at reducing the cost per peak watt. A cost reduction means narrowing the gap between photovoltaic and conventional power sources for many applications including water pumping.

Several authors have discussed the operational behaviour of the PVPWPS. Leguerre and M. Lascaud [1] studied the daily behavior of PVPWPS constituted from a centrifugal pump, a permanent magnet DC motor in direct coupling with silicon solar cells panels analytically [1]. Cirri and Maltagliati investigated the efficiency of the solar pump system without electrical storage [2]. [3 - 9] illustrate the using of PVPWPS, but by different types and other methods.

This paper suggests the operational behaviour models of four different aggregates of the PVPWPS. The results obtained of these models are compared to those obtained from the experimental data. The experimental data of this aggregation is modeled by linear and nonlinear mathematical expressions.

2-SYSTEM PERFORMANCE ANALYSIS

The investigated PVPWPS (Fig.1) takes one of the following configuration:

- a-The motor -pump set supplied from the PVCA directly ;
- b-The motor-pump set supplied from the PVCA through SB ;
- c-The motor-pump set supplied from the PVCA through the controller, and
- d-The motor-pump set supplied from the PVCA through SB and controller.

Performance analysis of these configurations is as follows :

2.1-Performance analysis of the motor pump set supplied directly from the PVCA (Fig.2).

The relation between terminal voltage V_L , current I_L and back e.m.f. E of the motor is

$$V_L = E + I_L R_a \quad (1)$$

where R_a is the armature resistance of the motor .

The back e.m.f E is

$$E = C \omega \quad (2)$$

where C is a constant and ω is the angular speed of the motor -pump set. Substituting from (2) in (1)

$$V_L = I_L R_a + C \omega \quad (3)$$

The torque equation of the motor is

$$T = C I_L \quad (4)$$

The torque of the centrifugal pump is given as

$$T = A \omega^2 \quad (5)$$

where A is a constant.

From eqns. (4) and (5)

$$\omega = \sqrt{C \cdot I_L / A} \quad (6)$$

Substituting from (6) in (3)

$$V_L = I_L R_s + \left(\frac{C}{A} I_L \right)^{1/2} \quad (7)$$

I-V characteristics of the PVCA is expressed as:

$$V_L = -I_L R_s - K_c \ln \left(\frac{I_{ph} - I_L + I_0}{I_0} \right) \quad (8)$$

where

V_L : terminal voltage, V; I_L : load current, A;
 R_s : array series resistance, Ω ; K_c : constant;
 I_{ph} : the photogenerated current, A; and
 I_0 : the reverse saturation current, A;

The operating points of the motor-pump set at different solar radiation levels is determined from Eq. (7) and Eq. (8) and revealed in Fig. 3.

From the operating points (V_L, I_L) , the motor input electric power

$$P_L \text{ is } P_L = I_L V_L \quad (9)$$

and the flow rate of the pump Q is

$$Q = P_h / C_t H_a \quad \text{lit./sec.} \quad (10)$$

where P_h : the pump hydraulic power input = $P_L - I_L R_s$;

C_t : a constant and = 9.81;

H_a : the total effective head (counting for the pump efficiency and all losses in the hydraulic circuit), meters.

2-2. Performance analysis of motor-pump set powered through SB

In this configuration, the motor-pump set is supplied from the PVCA through the SB as revealed in Fig. 4. The I-V characteristic of SB is represented by the expression:

$$V_L = B_1 \rho + B_2 = I_L R_b \quad (\text{charging/discharging}) \quad (11)$$

where B_1 & B_2 are constants; ρ : battery state of charge;

R_b : charging or discharging resistance of the battery, Ω .

If the SB is in charging mode the PVCA supplies the SB and the motor-pump set. But, when the SB is in discharging mode, the SB and PVCA supply the motor-pump set. Fig. 5 shows the operation points of SB and the motor-pump set in the charging/discharging modes of SB.

2-3. Performance analysis of the motor-pump set supplied through the controller.

Fig. 6 illustrates a motor-pump set powered from PVCA through a

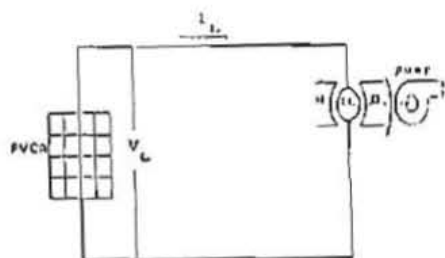


Fig. 2 A motor-pump set powered directly from PVCA.

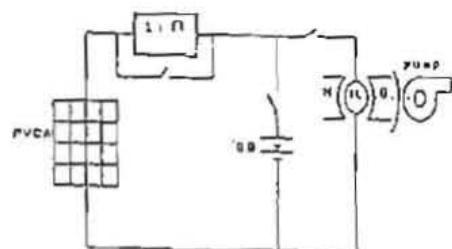


Fig. 1 Main components of PVWPS

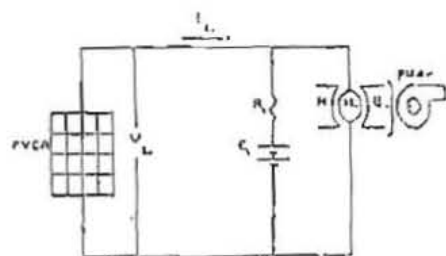


Fig. 4 Powering the motor-pump set through a SB

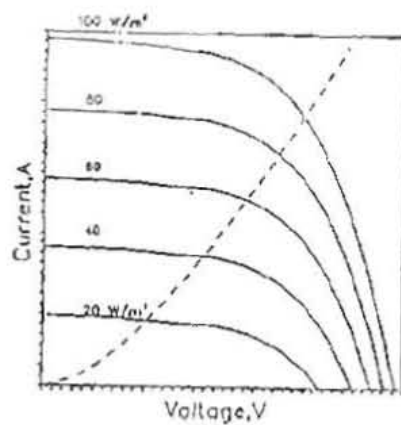
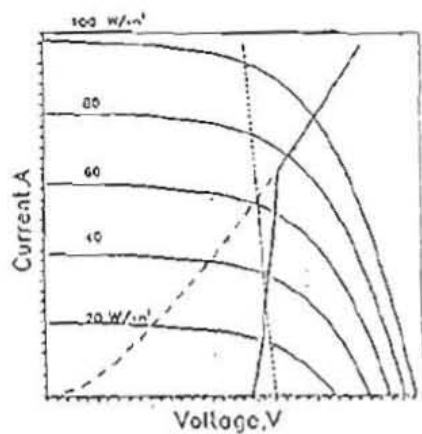
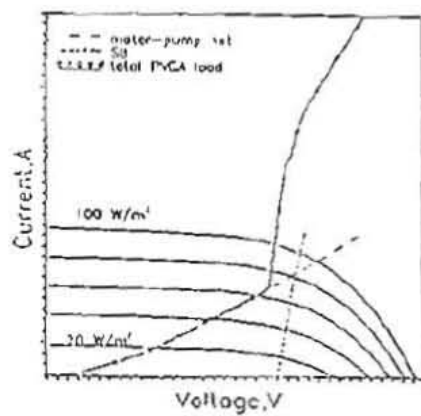


Fig. 3 Operation points of motor-pump set at different radiation levels



b- The SB in discharging mode



c- The SB in charging mode

Fig. 5 The operating points of the SB and motor-pump set in charging/discharging modes

controller. For maximum utilization of the solar cells, the matching is accomplished by incorporating into the system an electric control device, a maximum power point tracker (MPPT). The MPPT may be viewed as a time-varying transformer. The transformation ratio (n) is changed electronically, corresponding to the variations in the load operating point due to the fluctuations of solar radiation level.

The operation voltage (V_L) and current (I_L) are given by the following relations:

$$V_L = n V_M \quad \text{and} \quad I_L = I_M / n \quad (12)$$

where, V_M and I_M are the voltage and current of the maximum operating power, respectively.

Substituting from Eq. (12) in Eq. (1),

$$n V_M = I_M R_a / n + E \quad \text{Or}$$

$$n^2 V_M - n E - I_M R_a = 0 \quad (13)$$

From Eq. (13), the transformation ratio is

$$n = \{ E + (E^2 + 4 R_a P_M)^{0.5} \} / 2 V_M \quad (14)$$

where $P_M = V_M I_M$.

The operation voltage and current of the motor-pump set can be calculated as follows:

Multiplying both sides of Eq. (1) by I_L :

$$I_L V_L = I_L R_a + I_L E$$

Since $I_L V_L = I_M V_M = P_M$

So $P_M = I_L^2 R_a + E I_L$ and

$$R_a I_L^2 + E I_L - P_M = 0 \quad (15)$$

From (15), the operation current, I_L , is

$$I_L = [-E + (E^2 + 4 R_a P_M)^{0.5}] / 2 R_a \quad (16)$$

From Eq. (2) and Eq. (6)

$$I_L = (A / C) \omega^2 = (A / C^3) E^2 \quad (17)$$

By equalizing the right hand sides of Eq. (16) & Eq. (17):

$$AE^2 / C^3 + E / 2 R_a - (E^2 + 4 R_a P_M)^{0.5} / 2 R_a = 0 \quad (18)$$

2-4. Performance analysis of a motor-pump set powered through SB and controller

This situation is illustrated in Fig.7. The e.m.f., E_{eq} , and resistance, R_{eq} , across the two points A and B are:

$$E_{eq} = (E_b R_a + E r_b) / (R_a + r_b) \quad (19)$$

$$R_{eq} = R_a r_b / (R_a + r_b) \quad (20)$$

The terminal voltage between A and B is

$$V_L = I_L R_{oq} + E_{oq} \quad (21)$$

Or from eq. (12)

$$nV_M = (I_M/n) R_{oq} + E_{oq} \\ V_M n^2 - E_{oq} n - I_M R_{oq} = 0 \quad (22)$$

Therefore, the transformation ratio is

$$n = \frac{E_{oq}}{2V_M} + \left[\frac{E_{oq}^2 + 4P_M R_{oq}}{2V_M} \right]^{0.5} \quad (23)$$

Multiplying both sides of Eq. (23) by I

$$I_L V_L = I_L R_{oq}^2 + I_L E_{oq}, \text{ or}$$

$$P_M = I_L R_{oq}^2 + I_L E_{oq}$$

$$\text{Also, } I_L = -\frac{E_{oq}}{2R_{oq}} + \left[\frac{E_{oq}^2 + 4R_{oq}P_M}{2R_{oq}} \right]^{0.5} \quad (24)$$

From eqns. (3) and (4)

$$I_L = A/C^3 E^2, \text{ and}$$

$$V_L = I_{L1} R_a + E = -r_b I_{L2} + E_b$$

$$\text{So, } R_a I_{L1} + E + r_b I_{L2} - E_b = 0 \quad (25)$$

Where $I_{L2} = I_{L1} - I_L$ during discharging ($V_L < E$)

$I_{L2} = I_L - I_{L1}$ during charging ($V_L > E$)

From Eqns (24) and (25)

$$\frac{A}{C^3} (R_a + r_b) E^2 + \frac{E_b R_{oq}}{2R_{oq}} - \frac{r_b}{2R_{oq}} (E_{oq}^2 + 4R_{oq} P_M)^{0.5} + E - E_b = 0 \quad (26)$$

As E can be determined from eq. (28), the current I_{L1} is:

$$I_{L1} = (V_L - E)/R_a$$

Therefore, the electric power input of the motor .P. is

$$P = I_{L1} V_L, \text{ Watts}$$

Water flow rate ,Q ,can be calculated as in Eq. (10).

3- MATHEMATICAL MODELS OF THE SYSTEM PERFORMANCE

A long series of experimental measurements has been produced. Too many data points of water flow rate for the four system configurations studied and at different operation conditions (day number, temperature, tilt angle, solar radiation level, and battery state of charge) have been recorded. A mathematical model, making use of this data base, is to be constructed. This model may be used to predict the value of Q at any operating conditions with sufficient accuracy.

Regression analysis has presented two alternatives to construct such intended model, namely

a-linear regression model , and b- nonlinear regression model
Linear regression model

The dependent variable, y, is related linearly to the independent

variables, x_i , by the following form :

$$Y = \sum_i a_i X_i + b \quad \text{where } a_i \text{ is the coefficient of the } i^{\text{th}}$$

independent variable and b is a constant.

In this study, the dependent variable Q is related to the independent variables R, S, T, n and p by the following equation :

$$Q = a + bR + cS + dT + en + fp$$

The coefficients a, b, c, d, e and f are estimated for the four system configurations. The precision of the model is measured by the regression multiplier RM which is defined as :

$$RM = \sqrt{1 - \frac{\text{sum of residuals square}}{\text{sum of observed values square}}}$$

or

$$RM = \sqrt{1 - \frac{\sum (y - y^*)^2}{\sum (y^*)^2}}$$

where y is the observed value of the dependent variable.

For the different configurations of the PVPWPS installed, these coefficients are tabulated as shown in table 1.

Nonlinear regression model

In spite the simplicity of the linear regression model, RM is fairly low in some configuration. For getting more precious model, nonlinear expected relations are used. The different coefficients are estimated from the nonlinear regression technique. To obtain most proper model, large number of guessed models are solved using this technique. The regression multiplier RM is estimated for each model. The model which has the highest RM is chosen. The PVPWPS either directly coupled or coupled through a controller has the same model.

This model is $Q = aR^b + c \sin 0.001(S + n + T + d)$ lit/Sec. The PVPWPS either coupled through a storage battery or through a controller and storage battery has the following model:

$$Q = aR^{0.7}p^{0.7} + b(p)^{R/100} + c \sin 0.001(S + n + d)$$

The coefficients of this model and its regression multiplier, RM , on installing it at El-Mansoura city are tabulated in table 2. It is evident that the regression multiplier of the nonlinear models are higher than that of linear ones. Therefore, the nonlinear models describe the PVPWPS performance more accurately.

4- RESULTS AND DISCUSSION

The results deduced from this comparison are summarized in the following :

1- In the PVPWPS including a SB, the battery state of charge, p , is considered one of the most effective factors. So, the value of p must be specified during testing.

2- For the directly coupled configuration, referring to Fig.8, it should be noticed that :

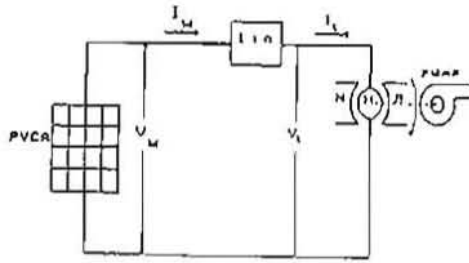


Fig. 6 Powering the motor-pump set through a controller

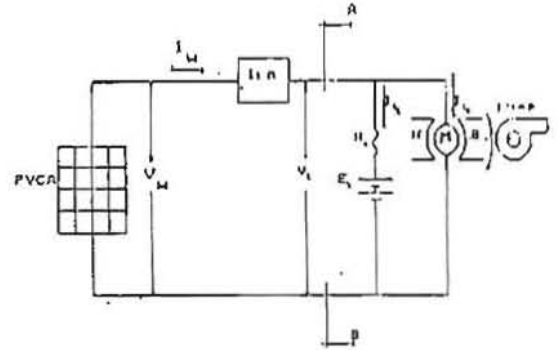
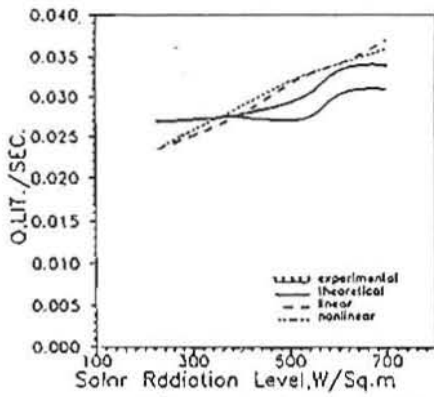
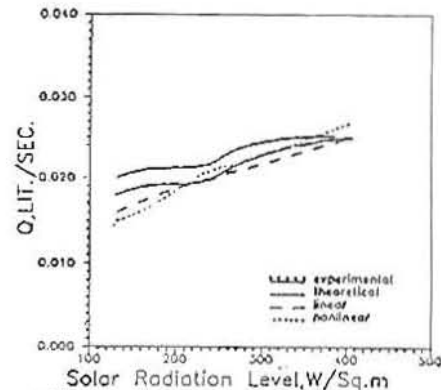


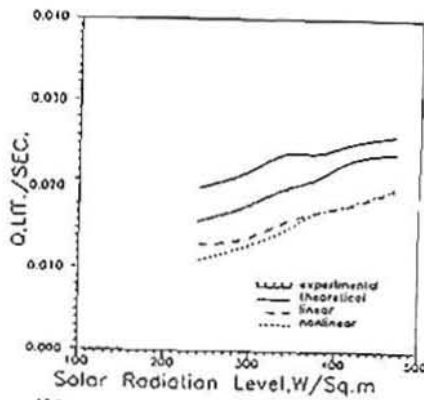
Fig. 7 Powering the motor-pump set through a 50 W controller



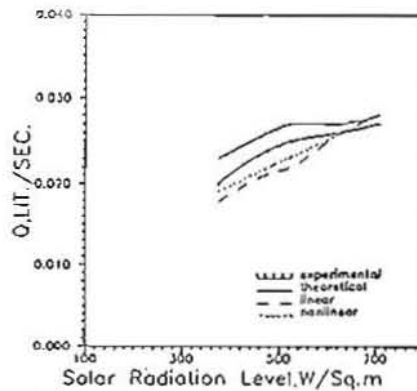
(i) $\alpha=31.8^\circ$, $n=72$ and $T=22c^\circ$ (Winter)



(ii) $\alpha=31.8^\circ$, $n=113$ and $T=26c^\circ$ (Spring)



(iii) $\alpha=31.8^\circ$, $n=315$ and $T=26c^\circ$ (Autumn)



(iv) $\alpha=31.8^\circ$, $n=246$ and $T=31c^\circ$ (Summer)

Fig. 8 Comparing water flow rate obtained experimentally to that obtained by theoretical model, linear regression model & nonlinear regression model (PVPWPS directly coupled) i, ii, iii, iv

- i- The day number 72 is chosen to represent the system performance through winter season. Curves of linear and nonlinear models are very close to each other. Both of them result in values of Q less than that obtained experimentally for all solar radiation levels. However, Q increases with the increase of solar radiation level as expected.
- ii- The day number 113 is chosen to represent the system performance during the spring season. The experimental, theoretical, linear and nonlinear curves are approximate to each other and this approximation increases as the solar radiation level increases. Therefore, the two regression models describe the system performance with complete accuracy in this season. The theoretical curve is slightly higher than the other curves.
- iii- The day number 246 is chosen to represent the system performance during summer season. The convergence between the four curves is obvious and increases as solar radiation level increases. The linear and nonlinear models curves may be viewed to be identical.
- iv- The day number 315 is chosen to represent the system performance during autumn season. Water pumping starts experimentally at solar radiation level of about 220 W/m^2 and below which there is no water pumping. There is a convergence between linear and nonlinear models.
- v- The average values of Q in autumn and spring are closed to each other and less than its value in summer. The maximum value of Q occurs in winter season at fairly high solar radiation level and low temperature.
- 3- For the configuration coupled through controller, shown in Fig.9, can be remarked that :
- i- There is a convergence between results calculated by linear and nonlinear models for all seasons.
- ii- The values of Q increase as the solar radiation level increases.
- iii- The minimum value of solar radiation level is required to start water pumping differs from one season to another. It reaches about 200 W/m^2 in summer season and less values for other seasons.
- iv- The average value of Q differs from one season to another. Its minimum value is in autumn and its maximum value is in winter.
- v- There is a similarity in PVPWS performance during spring, summer and autumn seasons.
- 4- For the configuration coupled through a SB, as indicated in Fig 10, can be observed that :
- i- There is a significant correlation between Q and battery state of charge .s .
- ii- The average value of Q is nearly the same for winter, spring and autumn seasons. It is higher than its corresponding value in summer season.
- iii- The system is always capable of water pumping as long as the battery is charged to an adequate level of charging.
- iv- There is a noticeable agreement between theoretical and experimental results.
- v- The nonlinear model curve is closer to the experimental curve than

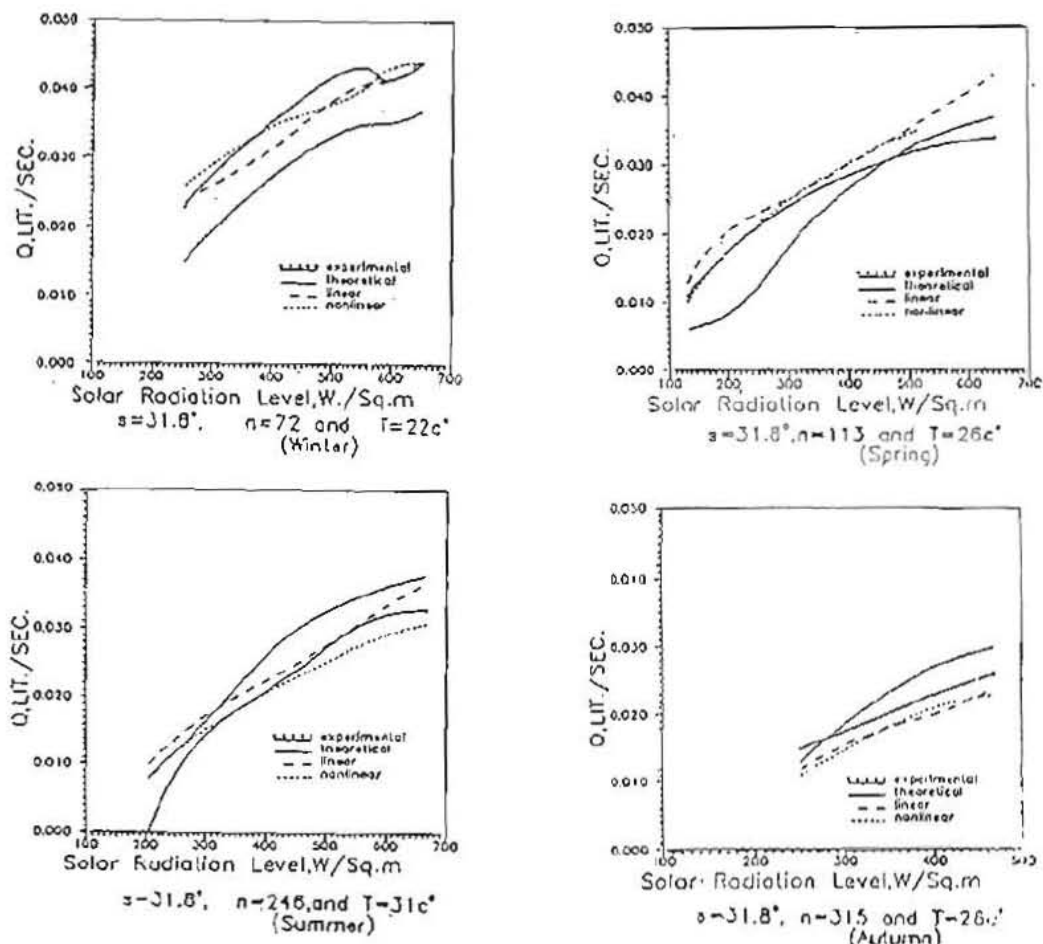


Fig. 9 Comparing water flow rate obtained experimentally to that obtained by theoretical model, linear regression model and nonlinear regression model (PVPWPS supplied through controller)

Table 1 Coefficients of the linear regression model and RM for the four different configurations of the Investigated PVPWPS

configuration	coefficient						Rn
	a	b	c	d	e	f	
directly coupled	0.0274	3.29E-5	1.2E-5	-4.49E-4	-3.7E-5	0	.853
through controller	0.0135	5.35E-5	-4.76E-6	1.93E-5	-4.79E-5	0	.836
through SD	0.0297	-1.21E-5	2.19E-5	-2.19E-4	6.25E-6	0.023	.74
through controller & SD	0.0017	-1.6E-5	3.89E-5	2.73E-4	3.48E-5	0.049	.84

the linear model. So, the linear model is less accurate in this case.
5- For the configuration coupled through a SB and controller, as demonstrated in Fig.11, it may be important to illustrate that :

- i- The performance is similar to the configuration of coupling through SB. Battery state of charge is still a significant affecting parameter.
- ii- The average value of Q is higher than its corresponding values in all seasons for the other three configurations.
- iii- The linear and nonlinear models oscillate around the experimental results with varying degrees of convergence .
- iv- The SB enhances and stabilizes the system performance .

General over view of Figs.8,9,10,11 and 12, can explore that :

- 1- PVPWPS performance is similar in spring and autumn seasons .
- 2- When SB is not contained in the configuration, water pumping may fail at low solar radiation levels. The minimum level required to start pumping differs from one season to another. This level is lower when a controller is included in the configuration .
- 3- The linear and nonlinear regression models describe the system performance with sufficient accuracy .

Fig.13 shows the effect of day number on flow rate Q. It can be concluded that :

- a- Water flow rate profile differs from one season to another. It depends on the climatic conditions of the season .
- b- Q has its highest values on days of low temperatures at the same operating conditions. The values of Q decrease as temperature increases.

Fig.14 illustrates the effect of tilt angle of the PVCA on the horizontal surface upon water flow rate. It deserves to be mentioned that :

- i- At the same operating circumstances, Q has its highest value tilt angle S of 31.8° . It is equal to the latitude of El-Mansoura, Egypt, where our laboratory is existed. Water flow rate at tilt angles of 11.8° and 51.8° which differs by $\pm 20^\circ$ from the latitude has less values than the corresponding values at the tilt angle of the latitude.
- ii- For tilt angles of 0° and 71.8° which differs by -31.8° and 40° respectively from the latitude, the values of Q are much less than those at $S = 31.8^\circ$. At $S = 71.8^\circ$, the system fails to pump water below solar radiation level of 200 W/m^2 while pumping has succeeded at this tilt angles. To obtain higher values of Q, it is recommended to operate the referred PVPWPS at tilt angle of latitude .

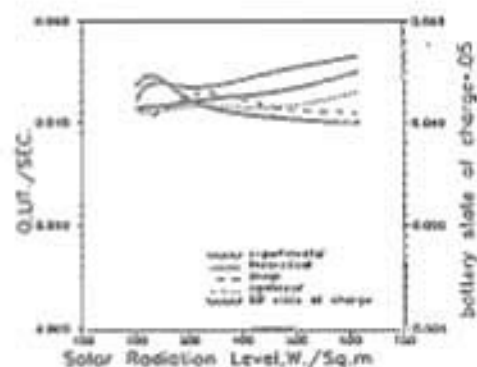
Fig.15 shows the effect of battery state of charge p on Q. It can be observed that any variation in p is accompanied by a greater change in the values of Q at the same conditions. This reflects the significant effect of the battery state of charge, if the SB is included, on the system performance .

5- CONCLUSIONS

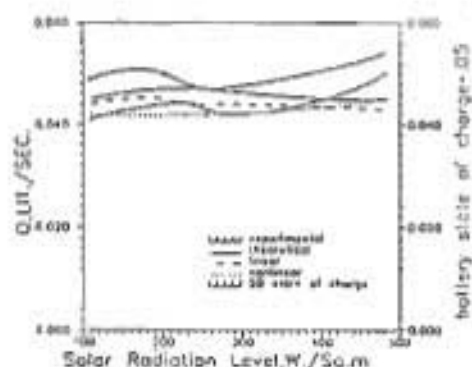
The performance of photovoltaic powered water pumping system (PVPWPS) is tested and analyzed at El-Mansoura city, Egypt. The system

Table 2 Coefficients and Rm of nonlinear models

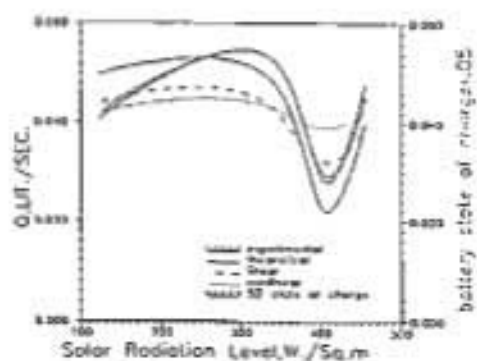
configuration	coefficients				Rm
	a	b	c	d	
directly coupled	0.113	0.07043	0.1593	4124.06	0.92
through controller	0.3100	0.04813	0.394	4315.25	0.91
through SB	3.846E-3	0.04533	-4.97E-3	1401.21	0.88
through SB&controller	4.007E-3	0.04579	-5.53E-3	1400.50	0.87



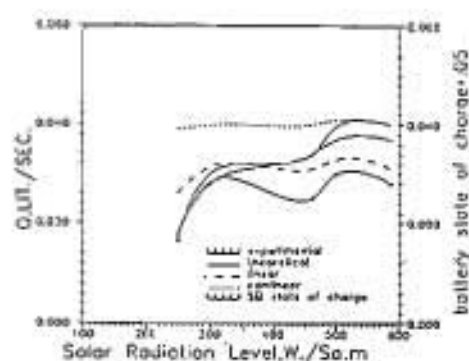
$\alpha=31.8^\circ$, $n=72$ and $T=22^\circ\text{C}$
(Winter)



$\alpha=31.8^\circ$, $n=113$ and $T=26^\circ\text{C}$
(Spring)



$\alpha=31.8^\circ$, $n=315$ and $T=26^\circ\text{C}$
(Autumn)



$\alpha=31.8^\circ$, $n=223$ and $T=30^\circ\text{C}$
(Summer)

Fig.10 Comparing water flow rate obtained experimentally to that obtained by theoretical model, linear regression model, nonlinear regression model (PVPKPS supplied through SB)

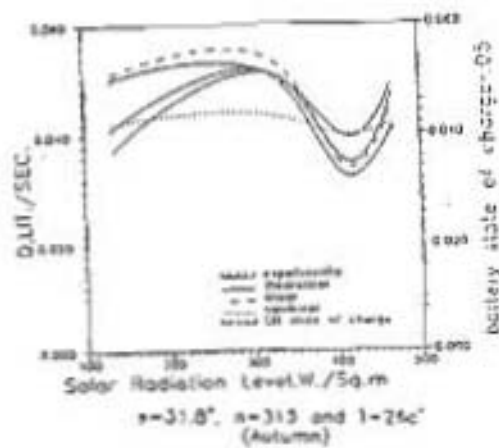
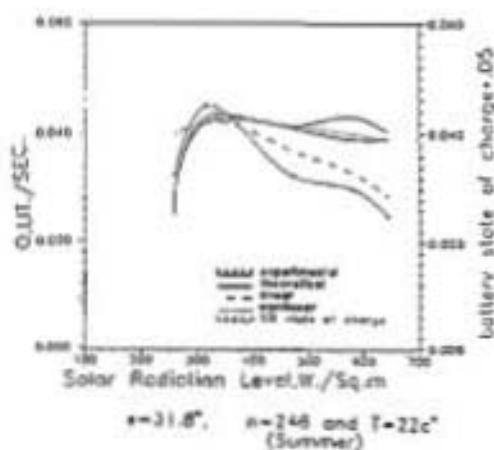
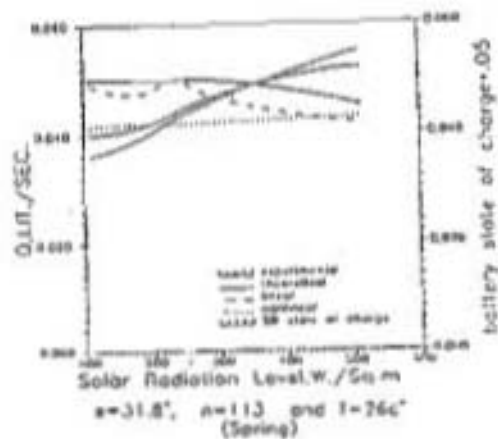
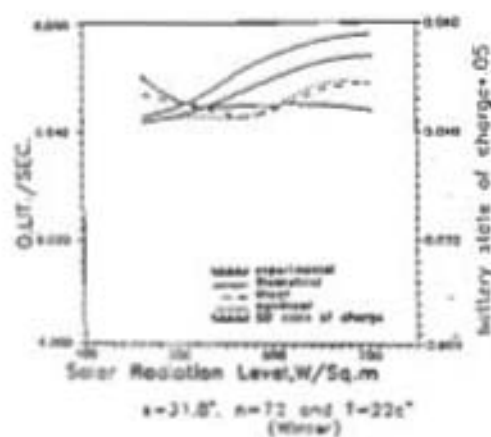
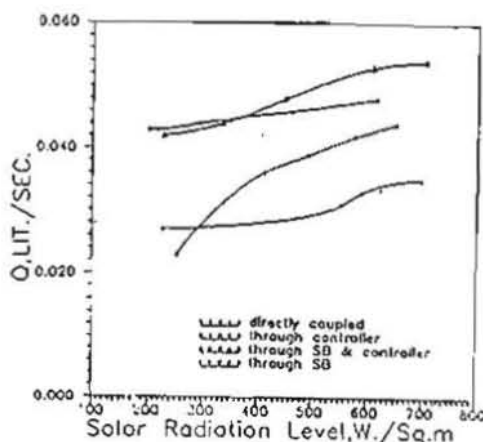


Fig.11 Comparing water flow rate obtained experimentally to that obtained by theoretical model, linear regression model & nonlinear regression model (PVPePS supplied through SB¢rififer)



$n=72$, $\beta=31.8^\circ$ and $T=22^\circ\text{C}$
 Fig. 12 Comparing PVPWPS performances
 for different configurations

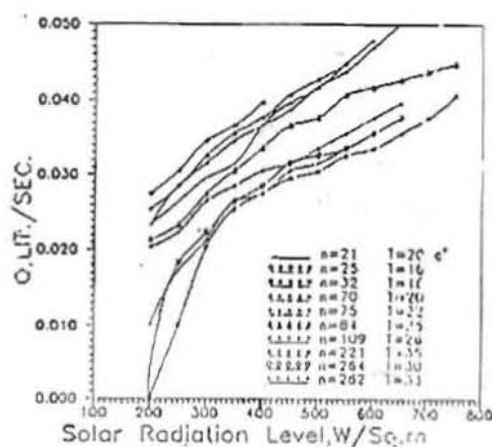


Fig. 13 Effect of day number on flow rate
 at $\beta=31.8^\circ$ (PVPWPS supplied through
 controller)

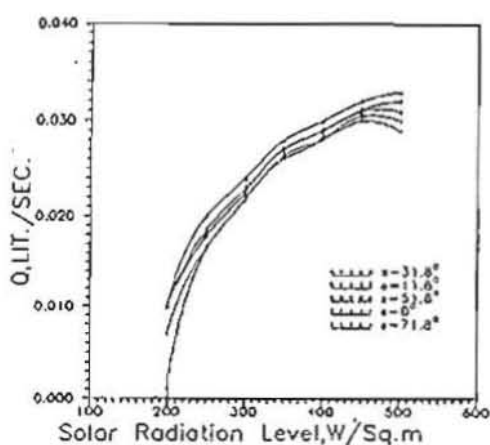


Fig. 14 Effect of tilt angle on flow rate at
 $n=320$ and $T=28^\circ\text{C}$
 (PVPWPS supplied through controller)

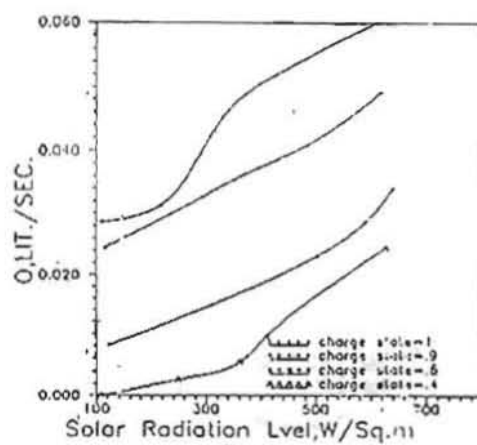


Fig. 15
 Effect of battery state of charge on flow
 rate (PVPWPS supplied through SA)

included a photovoltaic cells array PVCA, a controller, a storage battery and a permanent magnet DC motor driving a centrifugal pump. Four different system configurations were studied. Flow rate has been measured experimentally and evaluated theoretically. Mathematical models have been suggested to describe the system performance. These models may be exploited to estimate the water flow rate at any operating conditions. Results show that there is an obvious agreement between the values of water flow rate recorded experimentally and calculated theoretically. The suggested models are accurate enough to predict the system performance. The water flow rate increases with the increase of insolation. The minimum insolation is required to start water pumping differs from one season to another due to the variation in climatic conditions. This value is reduced by introducing the controller in the system configuration as a matching device. The controller improves also the values of water flow rate at the same operating circumstances. When SB is connected to the system, the system can start pumping regardless the insolation value as long as the storage battery is adequately charged. The connection of storage battery increases the values of water flow rate also. The system performance is very similar during spring and autumn seasons. The factors effect on the system performance has been studied. The tilt angle equating the latitude (31.8°) has been found as the optimum tilt angle. Battery state of charge has a significant effect on water flow rate produced by the system.

6- REFERENCES

- [1] J.R. Leguerre and M. Lscaud, "An Analytical Approach of a Photovoltaic Water Pumping System", Rabat -Maroc, 1981.
- [2] U. Cirri and M.M. Maltagliati, "Operation of Solar Pump System Without Electrical Storage", Solaris S.P.A, via C. Bini, 44 Firenze, Italy, 1984.
- [3] Dr. E. Picmaus and I. Franx, "Improvements of Efficiency of Solar Powered Pumps", N.V. Philips Gbellampenfabrieken, Eindhoven, 1983.
- [4] D.L. Pulfery, P.R.B. Ward and W.G. Dunford, "A Photovoltaic-Powered system For Medium-Head Pumping", Solar Energy, Vol. 38, No. 4, pp. 255-265, 1987.
- [5] B. Herrman, H. Karel and G. Lehn, "Realistic Indoor Testing of Photovoltaic Water Pumping System", Solar Energy, Vol. 38, No. 4, pp. 275-279, 1987.
- [6] W.Z. Fam and M.K. Blachender, "Dynamic Performance of a DC Shunt Motor Connected to a Photovoltaic Array.", IEEE Transactions on Energy Conversion, Vol. 3, No. 3, September 1988.
- [7] J. Applbaum and M.S. Sarma, "The Operation of Permanent Magnet DC Motors Powered by a Common Source of Solar Cells.", IEEE Transaction on Energy Conversion, Vol. 4, No. 4, December 1989.
- [8] M. Mahmoud, "Experience Results and Techno-Economic Feasibility of Using Photovoltaic Generators Instead of Diesel Motors for Water Pumping From Rural Desert Wells in Jordan.", IEE Proceedings, Vol. 137, Pt. 6, No. 6, November 1990.
- [9] Z.M. Salameh and F. Dagher, "The Effect of Electrical Array Reconfirmation on the Performance of a PV-Powered Volumetric Water Pump.", IEEE Transactions on Energy Conversion, Vol. 5, No. 4, Dec., 1990.